Available online at www.sciencedirect.com
ScienceDirect
Remote Sensing of Environment 112 (2008) 1912–1926
Remote Sensing of Environment
www.elsevier.com/locate/rse

Remote sensing of native and invasive species in Hawaiian forests

Gregory P. Asner [a,*], Matthew O. Jones [a], Roberta E. Martin [a], David E. Knapp [a], R. Flint Hughes [b]

[a] Department of Global Ecology, Carnegie Institution, 260 Panama Street, Stanford, CA 94305 USA
[b] Institute for Pacific Islands Forestry, Pacific Southwest Station, U.S. Forest Service, 60 Nowelo Street, Hilo, HI 96720 USA

Received 26 October 2006; received in revised form 25 January 2007; accepted 13 February 2007

Abstract

Detection and mapping of invasive species is an important component of conservation and management efforts in Hawai'i, but the spectral separability of native, introduced, and invasive species has not been established. We used high spatial resolution airborne imaging spectroscopy to analyze the canopy hyperspectral reflectance properties of 37 distinct species or phenotypes, 7 common native and 24 introduced tree species, the latter group containing 12 highly invasive species. Airborne Visible and Infrared Imaging Spectrometer (AVIRIS) reflectance and derivative-reflectance signatures of Hawaiian native trees were generically unique from those of introduced trees. Nitrogen-fixing trees were also spectrally unique from other groups of non-fixing trees. There were subtle but significant differences in the spectral properties of highly invasive tree species in comparison to introduced species that do not proliferate across Hawaiian ecosystems. The observed differences in canopy spectral signatures were linked to relative differences in measured leaf pigment (chlorophyll, carotenoids), nutrient (N, P), and structural (specific leaf area; SLA) properties, as well as to canopy leaf area index. These leaf and canopy properties contributed variably to the spectral separability of the trees, with wavelength-specific reflectance and absorption features that overlapped, but which were unique from one another. A combination of canopy reflectance from 1125–2500 nm associated with leaf and canopy water content, along with pigment-related absorption features (reflectance derivatives) in the 400–700 nm range, was best for delineating native, introduced, and invasive species. There was no single spectral region that always defined the separability of the species groups, and thus the full-range (400–2500 nm) spectrum was highly advantageous in differentiating these groups. These results provide a basis for more detailed studies of invasive species in Hawai'i, along with more explicit treatment of the biochemical properties of the canopies and their prediction using imaging spectroscopy.

Keywords: AVIRIS; Exotic species; Hawai'i; Imaging spectroscopy; Invasive species; Rainforest; Tropical forest

1. Introduction

Invasive species can alter the biological diversity and functioning of both land and aquatic ecosystems. Nowhere is this more obvious than in island ecosystems, many of which have undergone fundamental transformations caused by the introduction of new organisms (Sax et al., 2002; Vitousek et al., 1997). The Hawaiian Islands contain a wide range of bioclimatic zones and ecosystem types, from lowland rainforest to arid grassland, and the composition of nearly all Hawaiian ecosystems has changed following the proliferation of species from other parts of the world (Loope & Mueller-Dombois, 1989).

Introduced species do not always become invasive in their new environment. Here we define a species as invasive when it readily propagates across landscapes with or without being facilitated by human or natural disturbance (e.g. fire, deforestation, hurricanes). In the Hawaiian Islands, about 9000 organisms have been introduced, and approximately 120 plant species are considered highly invasive (www.hear.org). Although the life strategies that might make a plant invasive are hard to pinpoint, some basic characteristics correlated with the success of invasive plant species include: (1) an ability to grow through the native canopy, or in gaps, and eventually replace it (Vitousek & Walker, 1989; Yamashita et al., 2000); (2) alteration of fundamental ecosystem processes such as nitrogen (N) cycling (Ehrenfeld, 2003; Hughes & Denslow, 2005; Vitousek et al., 1987); and (3) an ability to alter

* Corresponding author. Carnegie Institution, 260 Panama Street, Stanford, CA 94305, USA. Tel.: +1 650 462 1047x200.
E-mail address: gpa@stanford.edu (G.P. Asner).

0034-4257/$ - see front matter © 2008 Elsevier Inc. All rights reserved.
doi:10.1016/j.rse.2007.02.043

disturbance regimes such as fire frequency (D'Antonio & Vitousek, 1992; Hughes et al., 1991). Resolving these characteristics, or their ultimate effects on ecosystem structure, is thus centrally important to any invasive species monitoring and mapping effort. However, no studies have demonstrated how this might be systematically accomplished.

Conceptual and operational approaches for remote detection and mapping of biodiversity and invasive species are currently lacking because we have a limited biophysical understanding of when remotely sensed signatures indicate the presence of unique species – native, introduced, or invasive – within and across ecosystems. By remote sensing signatures, we are referring generally to the spectral, temporal, angular, or spatial information contained in an observation, often obtained from airborne or spaceborne instruments. Here, we are focusing on the nadir (or near-nadir) spectral signatures in the 400 to 2500 nm wavelength region. For vegetation, these spectral signatures are determined by a combination of leaf biochemical and canopy structural properties including pigment, water and N concentrations, specific leaf area (SLA; leaf area per unit mass), canopy leaf area index (LAI), leaf angle distributions and stem/branch architecture (Jacquemoud et al., 1995; Myneni et al., 1989). Critically, the relative importance of these biochemical and structural properties is dependent upon measurement wavelength, pixel-size and ecosystem type (Asner, 1998). Currently, we do not know how to translate spectral signatures to species composition, but to do so, it may be important to relate spectral signatures to biochemical and structural information from which species composition might be inferred.

In broadleaf evergreen forests, leaf biochemistry, LAI and inter-crown gaps/shadows are the principle determinants of spectral signatures (Asner, 1998; Asner & Warner, 2003). However, at high spatial resolution (<5 m), biochemistry and LAI are the most important factors controlling spectral signatures of the sunlit portion of each observed tree crown (Zarco-Tejada et al., 2001). In the context of Hawaiian forest diversity and invasive species, we do not know if the spectral signatures of native and introduced trees are systematically different, and if so, the biochemical or structural basis for any observed differences. Field studies show that invasive tree species usually have higher growth rates than their native counterparts, often achieving these elevated growth rates via higher LAI and foliar efficiencies (Grotkopp et al., 2001; Gulias et al., 2003; Niinemets et al., 2002). Nitrogen, in combination with chlorophyll and accessory pigments, largely controls photosynthetic capacity and light-use efficiency (Evans et al., 2004; Reich et al., 1997; Wright et al., 2005), which are also often higher in invasive than in native Hawaiian species (Baruch & Goldstein, 1999; Durand & Goldstein, 2001). A combination of canopy LAI and leaf biochemical–physiological properties may thus indicate differences between native and introduced (or invasive) tree species.

Using high spatial resolution airborne imaging spectroscopy, we studied the spectral separability of native, introduced, and invasive tree species across a wide range of tropical and subtropical forest ecosystems in Hawai'i. We then collected field measurements of canopy LAI and top-of-canopy leaf pigment, N, and water content to interpret the spectra. We also assessed the spectral differences between N-fixing and non-fixing trees because N is a central determinant of the productivity and functioning of forest ecosystems. In doing so, we tested three hypotheses: (1) Spectral reflectance properties of introduced trees are both locally and regionally unique from that of native trees in Hawaiian forests. (2) The separability of native and introduced trees results from differences in concentrations of biochemicals and/or LAI expressed in specific wavelength regions of the reflectance spectrum. (3) Trees considered highly invasive are spectrally unique from that of introduced, non-invasive and native trees. Testing of these three hypotheses is requisite to any planned invasive species mapping and monitoring effort in Hawai'i.

2. Methods

2.1. Study sites and remote sensing

The Island of Hawai'i contains a globally-significant range of bioclimatic zones, including those that once contained native lowland, sub-montane and montane rainforests (Asner et al., 2005). These native forests are often dominated by the keystone Hawaiian tree species *Metrosideros polymorpha* (Dawson & Stemmermann, 1990; Stemmermann, 1983), although a variety of other native trees can also be found. In the past several hundred years, many exotic tree species have entered Hawaiian forests, resulting in a complex mosaic of tree compositions and forest structures in some areas (Loope & Mueller-Dombois, 1989). In more recent years, suburban development has encroached into nearly all forests on Hawai'i Island, further increasing the number of introduced trees at the expense of native tree canopies.

Our study took advantage of these mixed forest–suburban areas to develop a spectral database of the most common native and introduced forest tree species found in Hawai'i. In January and February 2005, the Jet Propulsion Laboratory (JPL) Airborne Visible and Infrared Imaging Spectrometer (AVIRIS) collected imagery over 12 sites spanning a range of tropical and subtropical sites (Fig. 1). AVIRIS was flown at ~3000 m a.g.l., providing spectral data at ~3.0 m spatial resolution. Based on our knowledge of the regions covered, we searched for tree species that could be clearly identified in the AVIRIS imagery. A tree was included in the spectral database when it met the following criteria: (1) the canopy was easily identified in the imagery; (2) the canopy was at least five AVIRIS pixels in diameter; (3) the tree stem basal area at breast height was at least 300 cm^2 (or cumulative stem diameters at breast height exceeding 20 cm) and (4) no other trees or structures were casting shade on any portion of the candidate tree crown. These criteria ensured that we compared the spectral properties of trees with fully developed, sunlit crowns. For this initial study, we purposely excluded smaller canopies to control for the effects of tree size and crown development on the spectral data.

Our spectral database included a total of 37 distinct species or phenotypes, 7 native and 24 introduced tree species, the latter group containing 12 species deemed highly invasive (Table 1; www.hear.org). There was one native N-fixing species *Acacia*

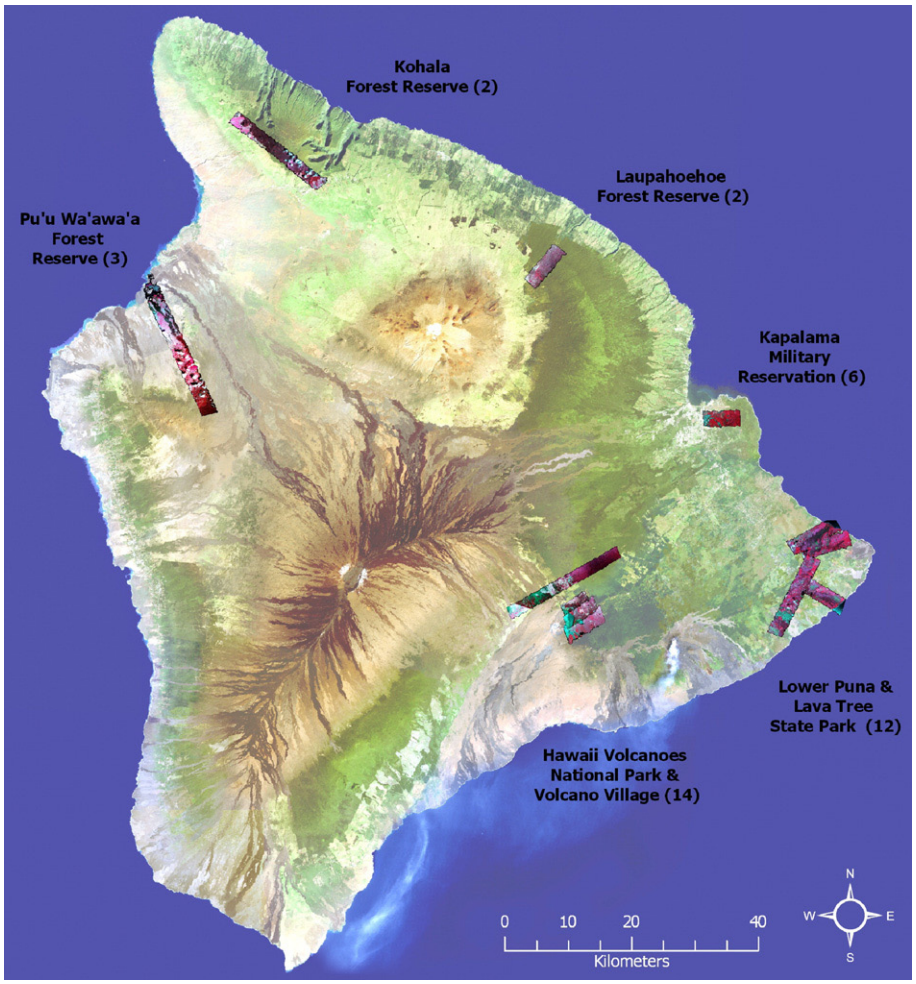

Fig. 1. Hawai'i Island showing the location of AVIRIS flight lines covering 35,000 ha of tropical and subtropical forest. Parentheses indicate number of species studied within each flight line (see Table 1).

koa, and three introduced N-fixers including *Falcataria moluccana*, *Morella faya* (previously *Myrica faya*), and *Casuarina equisetifolia*. All species in the database were broadleaf evergreen trees with the exception of three needleleaf evergreen tree species: *Cryptomeria japonica*, *Juniperus bermudiana*, and *Podocarpus nerifolius*. Native *M. polymorpha* samples were selected from six distinct phenotypes found in differing substrate ages and climate zones. All species were identified using Wagner et al. (1999).

Our tree selection protocol also included the collection of *Metrosideros* samples in all major forested zones on Hawai'i Island. Doing so allowed us to compare this most common native tree species to neighboring introduced species, thus controlling for local variations in climate and substrate age (Vitousek, 2004). This procedure resulted in five localized pairs of *Metrosideros* and 1–13 introduced tree species, depending upon the specific site (Fig. 1, Table 2).

2.2. Image processing

We used the ACORN-5 atmospheric radiative transfer model (ImSpec Inc., Palmdale, CA) to convert radiance data to apparent surface reflectance, and to mask wavelengths from 1344–1408 and 1793–2008 nm, which are dominated by atmospheric water absorption. This resulted in 194 channels of useable data spanning the 400–2500 nm wavelength range. All ACORN simulations used a tropical atmosphere, water vapor retrieval using the 940 and 1140 nm absorption features, and a 250 km visibility (aerosol) setting. Preliminary geo-registration of all data was performed using the inertial navigation system data collected onboard the aircraft. The images were further ortho-rectified using Landsat GeoCover data (http://glcf.umiacs.umd.edu/portal/geocover/) and geographic information system (GIS) layers provided by the State of Hawai'i (http://www.hawaii.gov/dbedt/gis/).

Following image pre-processing, the spectra of the sunlit portions of the selected tree crowns were extracted. The spectral sampling is reported in Table 1 on a canopy area, rather than a tree number basis, because often it was not possible to know when a cluster of tree stems represented one or several individuals. In addition to the calibrated reflectance imagery, we also worked with the first- and second-derivative of the spectral signatures. These derivative spectra were calculated using single and double 3-point Lagrangian interpolation.

Table 1
Species comprising the AVIRIS spectral database for Hawaiian forests

Species	Type	Common name	Origin	Area	Forest type	Canopy area	MAP	Substrate age
Metrosideros polymorpha	H	Ohia	Hawaiian Islands	Kohala	Subtropical	143	2500	120,000–230,000
				Kohala	Subtropical	142	2500	120,000–230,000
				Puna	Tropical	139	2700	Historic
				HAVO	Subtropical	139	2200	200–750
				PWW	Subtropical	140	1000	1500–3000
				KMR	Tropical	140	2700	750–1500
				Laupahoehoe	Subtropical	145	2500	14,000–65,000
				Puna	Tropical	139	2700	Historic
Diospyros sandwicensis	H	Lama	Hawaiian Islands	Puna	Tropical	140	2700	200–400
Myrsine lessertiana	H	Kolea lau nui	Hawaiian Islands	HAVO	Subtropical	140	2200	200–750
Nestegis sandwicensis	H	Olopua	Hawaiian Islands	HAVO	Subtropical	143	2200	1500–3000
Pisonia brunoniana	H	Papala kepau	Hawaiian Islands	HAVO	Subtropical	141	2200	1500–3000
Sapindus saponaria	H	Soapberry	Hawaiian Islands	HAVO	Subtropical	135	2200	1500–3000
Cecropia obtusifolia	I	Guarumo	C. and S. America	Puna	Tropical	140	2700	400–750
				KMR	Tropical	140	2700	750–1500
Cryptomeria japonica	I	Tsugi pine	China and Japan	Kohala	Subtropical	144	2500	120,000–230,000
				Volcano	Subtropical	151	2200	400–750
Eucalyptus deglupta	I	Rainbow eucalyptus	W. Pacific Islands	Puna	Tropical	135	2700	Historic
Eucalyptus globulus	I	Blue gum	Australia	Volcano	Subtropical	137	2200	400–750
Ficus benjamina	I	Weeping fig	S. Asia and Australia	Puna	Tropical	134	2700	200–400
Ficus elastica	I	Rubber tree	India and S. Asia	Puna	Tropical	135	2700	200–400
Ficus microcarpa	I*	Chinese banyan	India, S. China and Australia	Puna	Tropical	133	2700	400–750
				Puna	Tropical	134	2700	Historic
Fraxinus uhdei	I	Tropical ash	Mexico	Laupahoehoe	Montane	138	2500	14,000–65,000
				Volcano	Subtropical	137	2200	400–750
Grevillea robusta	I*	Silver oak	Australia	PWW	Subtropical	134	1000	1500–3000
Juniperus bermudiana	I	Bermuda juniper	S. America	Volcano	Subtropical	86	2200	400–750
Macaranga mappa	I*	Parasol leaf tree	Solomon Islands	KMR	Tropical	140	2700	750–1500
Magnolia grandiflora	I	Southern magnolia	N. America	Volcano	Subtropical	43	2200	400–750
Mangifera indica	I	Mango	Asia	KMR	Tropical	140	2700	750–1500
Melastoma Candidum	I*	Asian melastoma	Pacific Rim	KMR	Tropical	140	2700	750–1500
Podocarpus neriifolius	I	Brown pine	Pan-tropical	Volcano	Subtropical	42	2200	400–750
Psidium cattleianum	I*	Strawberry guava	S. America	KMR	Tropical	140	2700	750–1500
Schefflera actinophylla	I*	Octopus tree	Australia	Puna	Tropical	144	2700	750–1500
Schinus molle	I*	California pepper	S. America	PWW	Subtropical	137	1000	1500–3000
Spathodea campanulata	I*	African tulip	Africa	Puna	Tropical	136	2700	400–750
Tibouchina granulosa	I*	Glory tree	S. America	Volcano	Subtropical	135	2200	200–750
Trema orientalis	I*	Gunpowder tree	Asia and Pacific Islands	Puna	Tropical	136	2700	400–750
				Puna	Tropical	136	2700	200–400
Acacia koa	HN	Koa	Hawaiian Islands	HAVO	Subtropical	139	2200	200–400
				HAVO	Montane	141	2200	5000–10,000
Casuarina equisetifolia	IN	Australian beefwood	Pacific Rim, S. Pacific	Puna	Tropical	143	2700	Historic
Falcataria moluccana	IN*	Albizia	Indonesia	Puna	Tropical	139	2700	750–1500
Morella faya	IN*	Firetree	Canary Islands	HAVO	Subtropical	140	2200	400–750

Origin, forest type, site (Fig. 1), cumulative canopy area of spectral measurement (m^2), mean annual precipitation (MAP; mm), and substrate age (years) are also shown. Species types are Hawaiian non-nitrogen-fixing (H), Hawaiian nitrogen-fixing, introduced non-nitrogen-fixing (I), and introduced nitrogen-fixing (IN). Asterisks (*) denote species that are highly invasive according to http://www.hear.org.

2.3. Field and laboratory measurements

For each tree canopy identified in the AVIRIS imagery, we collected LAI measurements using a plant canopy analyzer (LAI-2000; Licor Inc., Lincoln, NE). The LAI estimates were made under diffuse sky conditions as required by the instrument data processing algorithms (Welles & Norman, 1991). A 50% optical block was used to mask the operator. An open sky measurement was collected followed by 12 under-canopy measurements. The LAI-2000 sensor head was oriented in the direction of the main stem from a position 30–50 cm within the edge (drip line) of the tree crown.

Leaves were collected from upper, full-sunlight positions in each tree canopy using a shotgun, slingshot or pole-clippers. Between 15 and 30 leaves were obtained from each canopy, and a sub-sample of six leaves were immediately stabilized in the field using liquid nitrogen, for subsequent analysis of pigment concentrations. The remainder of the sample was stored in polyethylene bags on ice for transport to a nearby laboratory. The samples were then weighed and scanned for leaf area. Foliar samples were oven-dried at 70 °C for at least 72 h and weighed for determination of SLA ($cm^2\ g^{-1}$). Dried leaves were ground in a 20-mesh Wiley mill, and subsets were analyzed for N and phosphorus (P) concentration using a Kjeldahl sulfuric

Table 2
Introduced species included in local spectral separability tests with native *Metrosideros polymorpha*

Site	Species	MAP	Substrate Age
HAVO and volcano	*Juniperus bermudiana* *Podocarpus neriifolius* *Magnolia grandiflora* *Fraxinus uhdei* *Eucalyptus globulus* *Cryptomeria japonica* *Morella faya* *Tibouchina granulosa*	2200–2400	400–750
Puna, lava tree and KMR	*Mangifera indica* *Casuarina equisetifolia* *Cecropia obtusifolia* *Ficus elastica* *Ficus benjamina* *Eucalyptus deglupta* *Psidium cattleianum* *Melastoma candidum* *Macaranga mappa* *Falcataria moluccana* *Ficus microcarpa* *Trema orientalis* *Schefflera actinophylla*	2600–2800	750–1500
Pu‘u Wa‘awa‘a	*Grevillea robusta* *Schinus molle*	1000	1500–3000
Kohala	*Cryptomeria japonica*	2500	120,000–130,000
Laupahoehoe	*Fraxinus uhdei*	2500	14,000–65,000

Ranges of mean annual precipitation (MAP) and substrate age (years) are also provided.

acid/cupric sulfate digest. Digests were analyzed using an Alpkem autoanalyzer (O–I Analytical, College Station, TX, USA).

Leaf pigment sub-samples were processed as follows: Frozen leaf discs (3 each, 0.79–1.13 cm^2 total area) were ground in 100% acetone in a chilled mortar, with a small amount of quartz sand and $MgCO_3$ added to prevent acidification. Following centrifugation for 3 min at 3000 rpm, the absorbance of the supernatant was measured using a dual-beam scanning UV–VIS spectrophotometer (Lambda 25, Perkin Elmer Ltd., Beaconsfield, United Kingdom). Chlorophyll a (chl-a), chlorophyll b (chl-b), and total carotenoid content were determined using a multi-wavelength analysis at 470, 645, 662 and 710 nm (Lichtenthaler, 1987; Lichtenthaler & Buschmann, 2001).

2.4. Statistical analysis

We first determined the spectral separability of four major groups of species: Hawaiian native non-N-fixing (H); Hawaiian native N-fixing (HN); introduced non-N-fixing (I); and introduced N-fixing (IN). Within the I+IN category, we compared those deemed highly invasive to those that have not rapidly proliferated in Hawaiian ecosystems (Table 1; www.hear.org; www.hawaii.gov/dlnr/dofaw/HISC/). We also compared the native, non-fixing species *Metrosideros* to I+IN in five distinct climate–substrate zones. All comparisons employed *t*-tests by wavelength for the reflectance data as well as the first-derivative (1st-d) and second-derivative (2nd-d) spectra. Whereas the reflectance spectrum includes the effects of both scattering (albedo) and absorption, the derivative spectra accentuate individual absorption features (Blackburn & Steele, 1999; Grossman et al., 1996; Jacquemoud et al., 1995; Li et al., 1993). In each species grouping, the combined variance was calculated to account for unequal variances encountered in the *t*-tests (Zar, 1999).

Relating the spectral signatures of species to their respective leaf biochemical and LAI properties requires an approach that can take full advantage of the continuous nature of the spectrum, rather than a band-by-band or per-feature analysis (Smith et al., 2003). We used a partial least squares (PLS) regression analysis method to explore the contributions of 10 biochemical constituents and LAI to the reflectance, 1st-d, and 2nd-d spectra of all species included in the study. Spectral weighting vectors generated by the PLS calculation correspond to features in the spectra related to each chemical constituent analyzed. The Prediction Residual Sum of Squares (PRESS) (Chen et al., 2004) statistic was calculated by reserving one of the 43 species' spectral samples, and predicting its chemical constituent using the PLS model created from the remaining samples (Coops et al., 2003). The number of factors used in each PLS analysis was determined by minimizing the PRESS statistic (Smith et al., 2003). A separate spectral weighting vector was generated for each eigenvector of each PLS model. We used an average of the spectral weighting vectors for each regression; the vector averaging was weighted in proportion to the amount that each factor reduced the PRESS statistic. In this way, the factors that contributed most to reducing the PRESS statistic were given the highest weight. The resulting values in the combined weighting vector were scaled from 0.0 to 1.0 to represent the relative influence that each spectral band provides in explaining the variation of each chemical constituent.

3. Results and discussion

3.1. Species group comparisons

Fig. 2 presents the mean and standard deviation spectra for Hawaiian native (H), introduced (I), Hawaiian N-fixing (HN), and introduced N-fixing (IN) species. It was immediately apparent that the introduced species had higher reflectance values in the near-infrared (750–1300 nm) wavelength region than the other groups. Moreover, the IN group had lower reflectance values in the 400–680 nm spectrum than non-fixing introduced species (I). Other than these few immediate observations, it was difficult to assess whether individuals or groups of species were spectrally unique, and thus a series of narrowing inter-comparisons were undertaken.

At the broadest scale of analysis, we found consistent, wavelength-specific differences between the H, I, HN, and IN groups (Fig. 3). In particular, spectral differences between H and I groups were highly significant across the 400–700 nm (upper-canopy pigments), 700–1350 nm (canopy water), and 1450–1900/2000–2500 nm (upper-canopy water and N) wavelength regions ($p<0.001$). A similar result was found in comparing HN

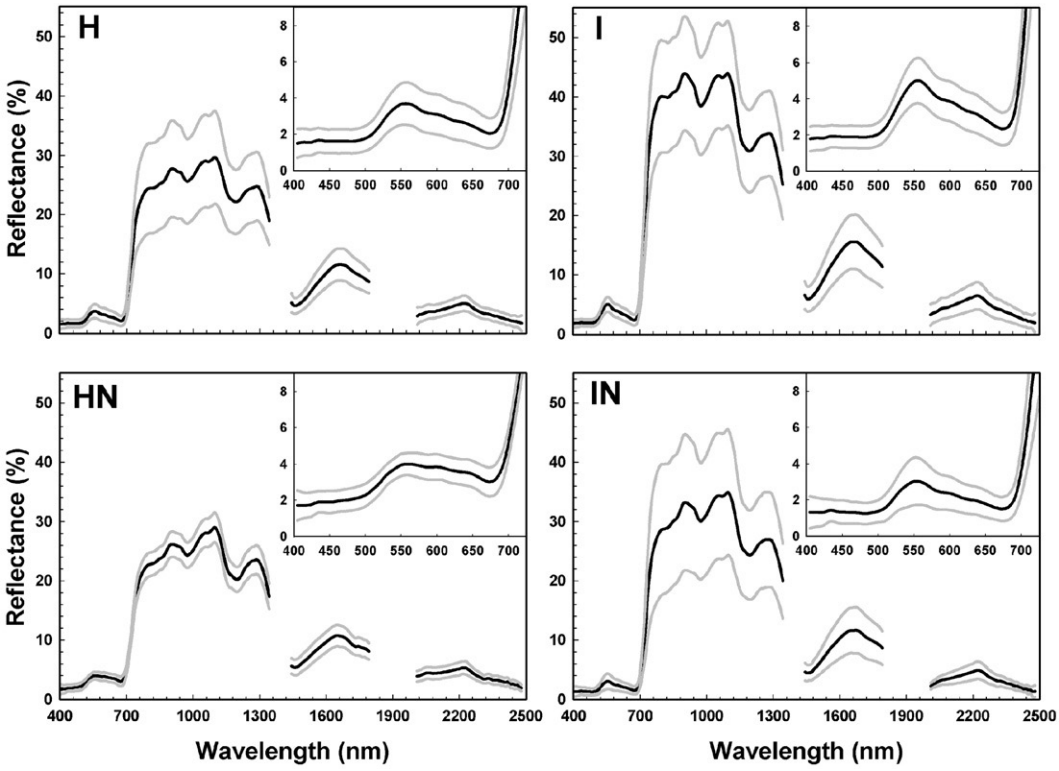

Fig. 2. Mean (±S.D.) spectral reflectance of Hawaiian non-nitrogen-fixer (H) and nitrogen-fixer (HN), and introduced non-fixer (I) and fixer (IN) species from Table 1. Insets show zoom of visible spectral region.

and I species groups, but with somewhat fewer wavelength-specific differences in the visible and shortwave-IR regions than were found in the H–I comparison. The spectral HN and IN signatures were significantly different in the visible (400–720 nm) and near-IR (750–1350 nm), but much less so in the shortwave-infrared (1450–1525 nm, 2000–2500 nm) spectral regions. Similarly, the H and IN groups were consistently unique in the visible and near-IR wavelength ranges. Other group

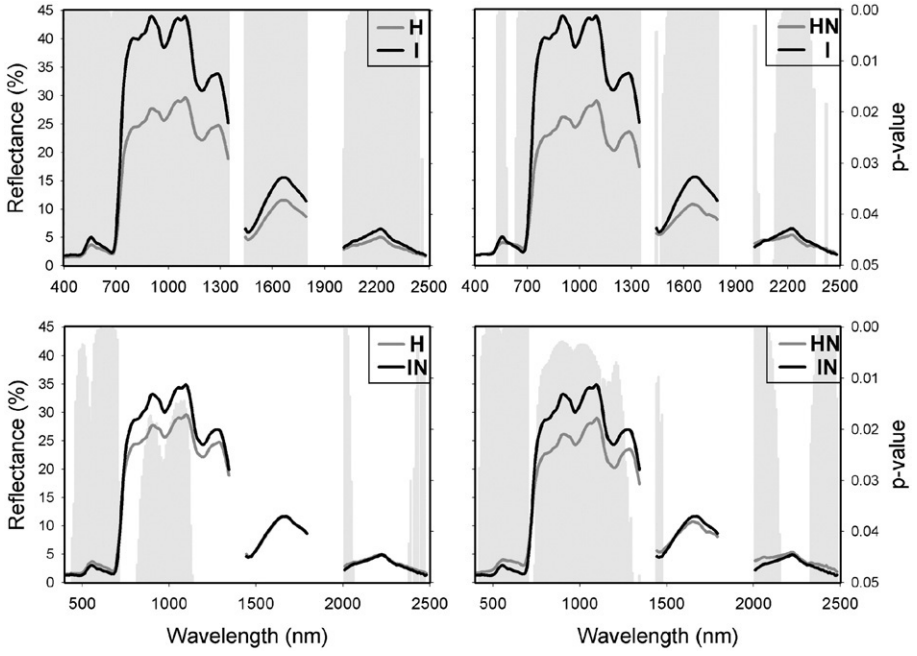

Fig. 3. Mean reflectance of Hawaiian non-fixing (H), Hawaiian nitrogen-fixing (HN), introduced non-fixing (I), and introduced nitrogen-fixing (IN) species, with band-by-band *t*-tests showing significant differences in grey bars (*p*-values ≤ 0.05).

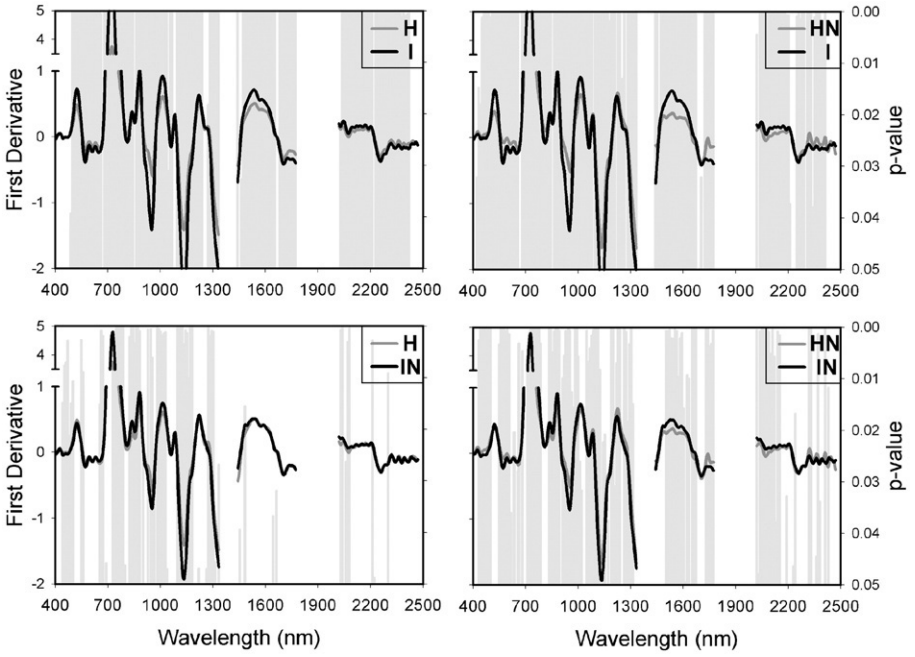

Fig. 4. Mean 1st-derivative spectra of Hawaiian non-fixing (H), Hawaiian nitrogen-fixing (HN), introduced non-fixing (I), and introduced nitrogen-fixing (IN) species, with band-by-band *t*-tests showing significant differences in grey bars (*p*-values ≤ 0.05).

combinations (I–IN and H–HN) showed variable separability in all spectral regions (data not shown).

Using 3-point Lagrangian interpolated 1st-d spectra, we found a variety of absorption features in the pigment (400–700 nm), canopy water (700–1300 nm), and leaf water (>1500 nm) wavelengths that were statistically unique among groups of native and introduced species (Fig. 4). For the H–I and HN–I comparisons, the 1st-d spectral differences were as abundant as those observed in the reflectance analyses of Fig. 3; however, the 1st-d spectra revealed a new set of features not identified in the reflectance data. In particular, 1st-d features associated with chl-a (<430 nm), chl-b (550–650 nm), and canopy water content (900–1250 nm) were statistically unique in the H–I and HN–I comparisons. H–IN and HN–IN groups were also highly separable using 1st-d spectral

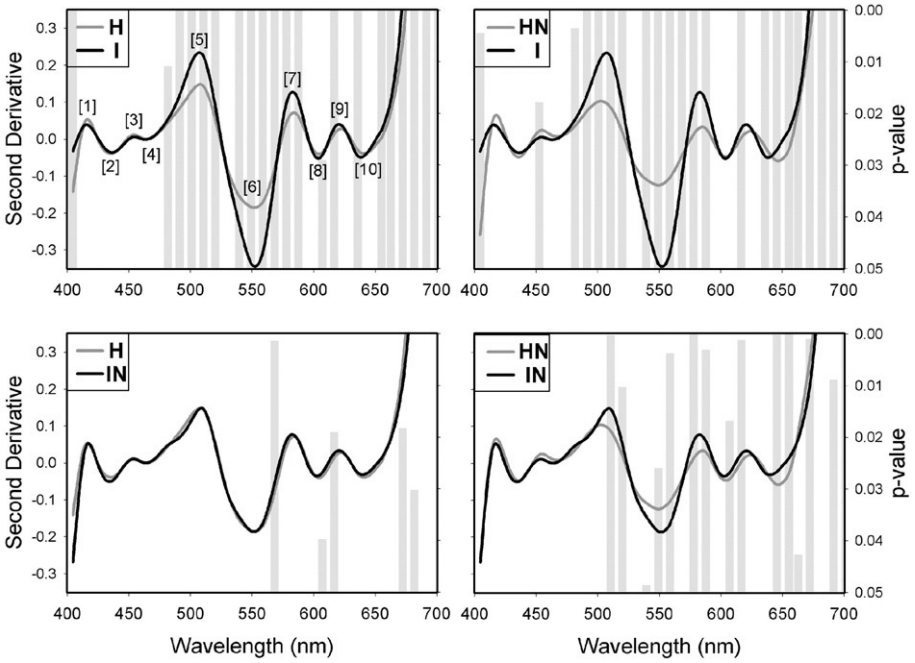

Fig. 5. Mean 2nd-derivative spectra (400–700 nm) of Hawaiian non-fixing (H), Hawaiian nitrogen-fixing (HN), introduced non-fixing (I), and introduced nitrogen-fixing (IN) species, with band-by-band *t*-tests showing significant differences in grey bars (*p*-values ≤ 0.05). Upper left panel also shows major pigment features most closely associated with [1–2] chl-a, [3–5] carotenoids, and [6–10] chl-a/b combinations.

features, which were variably spaced throughout the visible, near-IR, and shortwave-IR regions (Fig. 4).

Analysis of second- and high-order derivatives requires extremely high performance spectroscopy, rarely available from airborne instruments. Following the 2005 update of the AVIRIS sensor, the 2nd-d spectra were meaningful in our study. 2nd-d spectra isolate local changes in the shape of 1st-d spectra. A negative or positive peak in the 2nd-d spectrum indicates the location of a local minimum or maximum slope, respectively, in the 1st-d spectra. There were several spectral regions showing statistically different 2nd-d values among the four groups of species. Here, we display the detailed 2nd-d spectra in the visible wavelengths, where chl-a, chl-b, and carotenoids dominate (Fig. 5). H and I tree groups had significantly unique chl-a and chl-b features at 410, 430, and 600–690 nm. Carotenoid features centered at 510 and 550 nm were also highly unique. Very similar results were found for HN–I analysis. Few 2nd-d features were found to separate the H from IN groups, whereas the HN–IN comparisons showed a sparse distribution of statistically different 2nd-d features associated with chl-a, chl-b and carotenoids.

Since the visible portion of the spectrum is dominated by leaf pigment contributions from the top of the canopy (Blackburn & Steele, 1999; Zarco-Tejada et al., 2001), spectral derivatives are a good approach to isolate pigment expressions in this wavelength region, thereby minimizing other contributions from intra-canopy gaps and shadows (Sims & Gamon, 2002). Whereas the visible spectral range is dominated by leaf pigment constituents, spectral variations in the 750–2500 nm region are mostly driven by changes in leaf and canopy water content, with associated changes in LAI (Ceccato et al., 2001; Ustin et al., 2004). Our results showed that H–I and HN–I groupings were easily separable in the near-IR and shortwave-IR regions associated with water when reflectance and 1st-d spectra were compared (Figs. 3–4). These distinctions were lost when 2nd-d spectra were examined (data not shown).

Overall, this portion of our analysis suggested that remote sensing of Hawaiian native and introduced species is generically possible, and may best be achieved via a combination of reflectance and derivative-reflectance signatures. Notably, these analyses show that no single band or spectral region will provide universal separability of the four groups. Furthermore, the spectral separability of these four groups may rest on our ability to accurately measure spectroscopic signatures that allow high-order derivative analysis to isolate various pigment features.

3.2. Introduced vs. invasive species

We regrouped the spectral database of introduced tree species into those deemed highly invasive and those that have not proliferated in Hawaiian ecosystems (Table 1; www.hear.org; www.hawaii.gov/dlnr/dofaw/HISC/). We then carried out the spectral separability tests on these two distinct groups of plants. The results showed a very subtle, but highly significant, and nearly continuous spectral separation beginning at 1125 nm and continuing to 2500 nm (Fig. 6A). In these densely foliated

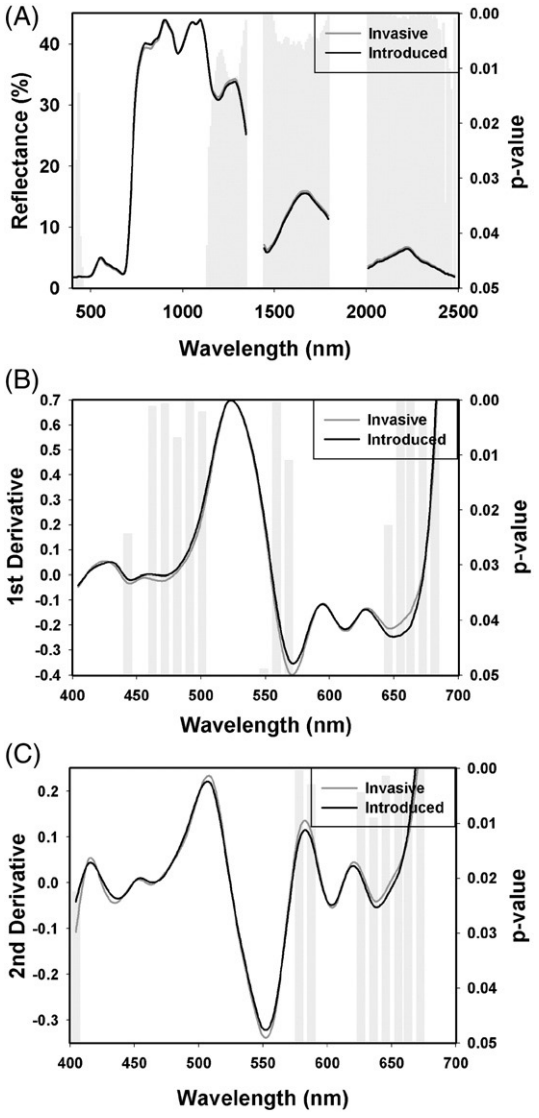

Fig. 6. (A) Reflectance, (B) 1st-derivative, and (C) 2nd-derivative spectra of highly invasive vs. other introduced tree species of Hawaiian tropical and subtropical forests, with band-by-band *t*-tests showing significant differences in grey bars (p-values < 0.05).

canopies, the 1125–2500 nm spectral range is foremost dominated by variations in canopy water content, but to varying canopy depths. For example, photons in the 1125–1300 nm range are efficiently scattered by foliage, resulting in a very deep "effective photon penetration depth" (EPPD), as described by Asner et al. (2006). As wavelength increases from 1300 nm, EPPD generally decreases, and thus the volume and mass of canopy water expressed in the spectrum decreases. This occurs because the EPPD is proportional to the single-scattering albedo of the foliage, which generally decreases with increasing wavelength (although there are local maxima near 1650 and 2200 nm). The net outcome of this phenomenon is that the amount of foliage that contributes to the AVIRIS reflectance spectrum is maximal in the 1125–1300 nm range, then decreases to a minimum at roughly 2000 nm and 2500 nm. This is critically important to interpreting near-IR/shortwave-IR signatures of closed-canopy forests, since

we are effectively sensing down to different levels into the canopy using the continuum spectrum.

In Fig. 6A, the small but statistically ($p<0.01$) higher 1500–2500 nm reflectances of the invasive species group indicates that their upper-canopy water content is lower, on average, than the remaining introduced species. This observation is strongly supported by measured differences in leaf thickness and water content between the introduced and invasive species. First, the SLA of invasive trees averaged 88.9 (±13.5) $cm^2\ g^{-1}$, or about 30% higher than that of other introduced species (69.4±10.6 $cm^2\ g^{-1}$) (*t*-test; $p<0.05$). Leaf equivalent water thickness (EWT), which is the product of leaf water concentration and (1/SLA), was 0.19 (±0.02) mm for invasives and 0.25 (±0.04) mm for other introduced trees (*t*-test; $p<0.05$). SLA and EWT are among the most important determinants of shortwave-IR signatures (Ceccato et al., 2001), and thus these field measurements (Appendix A) align well with our spectral results. SLA is, in turn, correlated with chl-a, chl-b, carotenoids and N per area (Reich et al., 1997; Wright et al., 2005), all of which were higher in the group of highly invasive species as compared to the other introduced species (*p*-values ranging from 0.01–0.05). Although we did not observe significant differences in the 400–700 nm reflectance spectra of introduced and invasive species, we did find highly significant differences in 1st-d and 2nd-d spectra that are closely linked to leaf pigments and N (Fig. 6B–C). We thus conclude that a combination of canopy brightness (albedo) in the 1125–2500 nm region associated with canopy water content, along with pigment-related absorption features (1st-d, 2nd-d) in the 400–700 nm range, is best for delineating invasive and introduced species.

3.3. Localized native-introduced species comparisons

At the local scale, there were consistent and highly significant spectral differences between the most common native tree *M. polymorpha* and neighboring introduced species (Fig. 7). In most sites, *Metrosideros* had a far lower reflectance in the 700–2500 nm range than did introduced trees. Analysis of 1st-d and 2nd-d spectra also highlighted a variety of absorption features separating *Metrosideros* from the introduced species (data not shown). In the visible spectral range, *Metrosideros* had a lower reflectance in three of the five sites. The exceptions were Laupahoehoe and Kohala Forest Reserves, the two highest fertility sub-montane sites (Crews et al., 1995; Herbert & Fownes, 1999). The driest site, Pu‘u Wa‘awa‘a (MAP=1000 mm yr^{-1}), had the lowest near-IR reflectances among all sites, yet the reflectance of *Metrosideros* remained

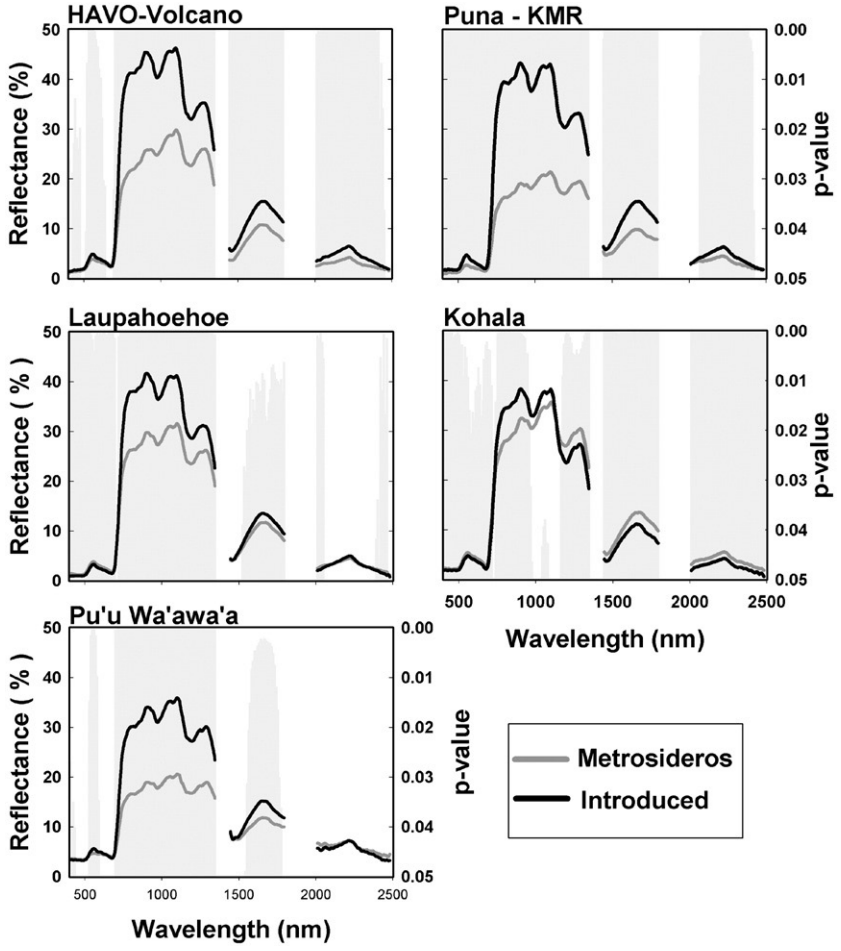

Fig. 7. Local-scale comparisons of the most common Hawaiian tree *Metrosideros polymorpha* and the introduced species listed in Table 2, with band-by-band *t*-tests showing significant differences in grey bars (*p*-values ≤ 0.05).

proportionally lower than the introduced species in that ecosystem. Overall, these results show that the Hawai'i's most common, and arguably one of the most important species for habitat (Vitousek, 2004), is readily separable from the various types and assemblages of introduced species found on the island. This is key to mapping efforts seeking to identify remaining *Metrosideros* trees deemed valuable to conservation management and ecological studies. Future studies will provide a more in-depth analysis of the spectral separability of individual species; here, we were mainly interested in understanding if the localized group of introduced trees is consistently different from *Metrosideros*.

3.4. Biochemical and structural contributions to spectral properties

Leaf pigments, canopy water and LAI are directly expressed in reflectance spectra spanning the 400–2500 nm wavelength region (reviewed by Ustin et al., 2004). However, linking our observed spectral differences between Hawaiian native, introduced, and invasive species (Figs. 3–7) to the chemistry is challenging because: (i) field-based sampling is inherently limited, and thus correlation analyses usually lack statistical power once the data are partitioned into groups of species; (ii) spectral absorption features are often overlapping, and are affected by more than one biochemical constituent; and (iii) spectral features are often subtle, and cannot easily be captured using band-by-band analyses (e.g., vegetation indices) or single feature-based spectral analyses (Clark et al., 2003). Our PLS regression analyses overcame several of these limitations to analyze the relative importance of spectral features for each biochemical and for LAI.

The relative weightings in Fig. 8 show how the reflectance spectra of all tree species contributed to the best prediction of their leaf and canopy properties. We found that the 750–1300 nm range dominated the canopy LAI prediction (Fig. 8A),

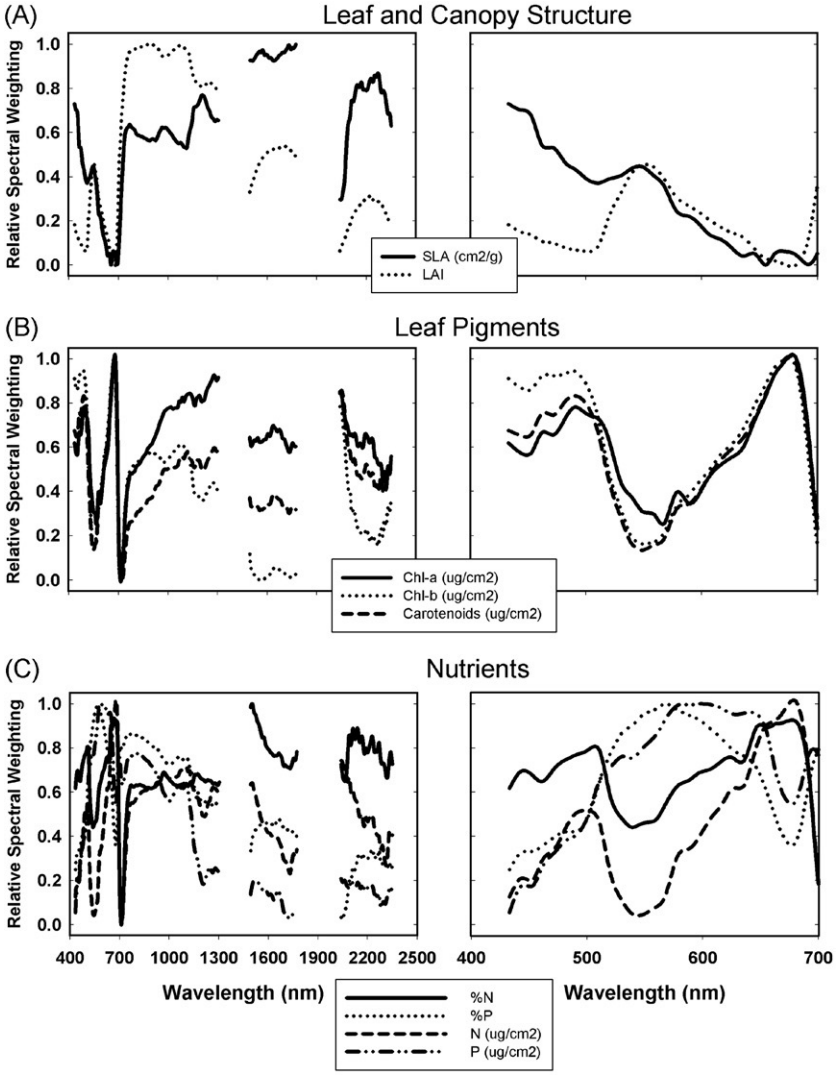

Fig. 8. Relative spectral weightings of (A) leaf SLA and canopy LAI; (B) leaf chl-a, chl-b, and carotenoids; and (C) leaf N and P, on AVIRIS reflectance spectra of all tree species in Table 1. The right panels show 400–700 nm zoom graphs of the left 400–2500 nm panels.

and that the relative weightings took the general shape of a canopy spectrum. This was expected because photons scatter more efficiently in the near-IR than in any other portion of the optical spectrum, mainly due to the scattering properties of the foliage. However, we were surprised to find that the 1500–2500 nm reflectance range was most important for predicting SLA. Predicting SLA is of great importance because this parameter is highly correlated with N, photosynthetic rates, and an enormous range of other plant characteristics that mediate ecosystem functioning (Niinemets et al., 2002; Reich et al., 1997; Wright et al., 2005). SLA is even linked to plant properties that predict invasiveness among species (Baruch & Goldstein, 1999; Rejmánek et al., 2005), as discussed in a previous section.

The relative prediction weightings for chl-a, chl-b, and carotenoids varied throughout the reflectance spectrum (Fig. 8B). In the visible region directly affected by pigment chemistry, there was a maximum weighting feature at 670 nm for all three constituents. There were also weightings in the near-IR and shortwave-IR regions that were important to the PLS regressions. However, these weightings are indirectly related to pigments via SLA since chl-a, chl-b, and carotenoids are expressed on a per-area basis here, and otherwise have no molecular interactions with radiation in the near-IR or shortwave-IR (Curran, 1989).

Similarly, leaf N and P were predicted by a combination of spectral reflectance features (Fig. 8C). The shortwave-IR was a major contributor to the prediction of leaf N concentration. There are protein-N absorptions at 1510, 1690, 1940, 1980, 2060, 2180, and 2300 nm in dried foliage (Curran, 1989), and in fresh foliage as well (Asner & Vitousek, 2005; Martin & Aber, 1997; Smith et al., 2003; Wessman et al., 1988), although to a much lesser degree due to water obscuring the absorption features associated with N. It is notable that shortwave-IR was more important in predicting leaf N concentration than N on a per-area basis, the latter measure including the effects of SLA. Since SLA was poorly correlated with %N in our study ($r=0.6$, $p=0.06$), there is an increased possibility that the protein-N bonds were, in fact, directly expressed in the shortwave-IR.

We also found that the visible region was a very strong contributor to N and P predictions, but interestingly, the relative weighting of the visible spectrum varied by constituent and unit of measure. The spectral reflectance weightings for leaf N on either a concentration or per-area basis (Fig. 8C) closely mirrored those of the leaf pigments (Fig. 8B), likely due to the stoichiometric balance between chlorophyll and N in plant leaves (Yoder & Pettigrew-Crosby, 1995). Surprisingly, the spectral weightings for P reached maxima in the 550–625 nm range (Fig. 8C), which was unique from all other plant properties that we tested. Since P is not directly expressed in the reflected solar spectrum, these weightings are probably indirectly linked to pigments, although the precise connection remains unclear.

PLS regression with 1st-d and 2nd-d spectra uncovered additional, subtle spectral features contributing to the leaf biochemical predictions. First-derivative weightings for SLA were concentrated in the visible and near-IR, with peaks at 520, 750, 870, 990 and 1210 nm (Fig. 9A). The latter three 1st-d features are associated with leaf water thickness, whereas the 750 nm feature is related to the red-edge. The 520 nm feature is difficult to assess, but it was completely out of phase with the 1st-d spectra weightings for pigments. The 1st-d spectral weightings for pigments reached maxima at 456, 480, 580, 600 and 640 nm (Fig. 8B). These are all generally related to pigment absorption peaks (Datt, 1998; Sims & Gamon, 2002), although not uniquely among the three pigments in our case. However, 2nd-d spectral weightings had definitive peaks at 450, 460, 500, and 510 nm associated with either carotenoids, chl-a, or a combination of these pigments (Gitelson et al., 2002). Other 2nd-d weighting maxima at 550, 560, 600, and 630 nm are linked directly to total chlorophyll content of leaves. We were not able to identify or interpret other 1st-d and 2nd-d weightings in the remaining portions of the spectra (1300–2500 nm and 700–2500 nm are omitted from Fig. 9B and C, respectively).

The key finding of the PLS study was that specific leaf biochemicals, SLA, and LAI are directly linked to the

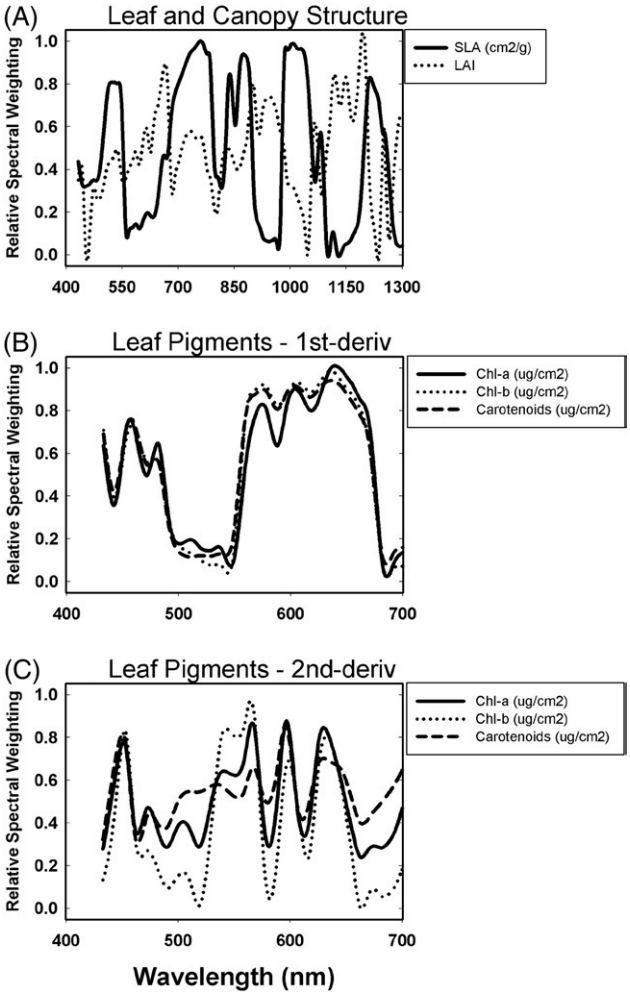

Fig. 9. Relative spectral weightings of (A) leaf SLA and canopy LAI; (B) leaf chl-a, chl-b, and carotenoids; and (C) leaf N and P, on AVIRIS derivative spectra of all tree species in Table 1. Panels (A) and (B) are 1st-derivatives; panel (C) contains 2nd-derivatives.

reflectance and derivative-reflectance features that make native Hawaiian, introduced and invasive species spectrally unique. No single biochemical or structural property determined the spectral signatures of these groups of species. All plant properties co-vary biochemically and ecologically, resulting in an ensemble of contributions that determined the spectra. Nonetheless, specific wavelength regions were dominated by particular leaf or canopy properties. Higher near-IR reflectances of introduced and invasive trees, as compared to native Hawaiian species (Figs. 3, 6–7), were driven by higher LAI values among the non-natives (Fig. 8A, Appendix A). Surprisingly, shortwave-IR reflectance signatures of the species (Figs. 3, 6–7) were largely determined by changes in upper-canopy SLA (Fig. 8A). Finally, the separability of species using derivative spectra (Figs. 5–6) was mostly driven by differences in pigment contents in the visible and SLA in the near-infrared (Fig. 9B,C).

Based on our collective findings here, as well as previous work (Baruch & Goldstein, 1999; Durand & Goldstein, 2001; Hughes & Denslow, 2005; Vitousek & Walker, 1989), we contend that there are systematic biochemical and structural differences among native and introduced tree species in Hawai'i. These differences are the direct expression of differing life strategies and functional properties among species. Moreover, these differences are linked both to the ecological success of a species and to its high-resolution spectral characteristics. These results thus pave the way for more detailed species-level studies, along with more explicit treatment of the biochemical properties of the canopies and their prediction using imaging spectroscopy.

4. Conclusions

Hawaiian ecosystems continue to undergo enormous changes in their composition and function caused by the spread of exotic species. Research, conservation and management efforts are calling for methods to map, monitor and predict the spread of new species, and to understand their impact on native ecosystems. Remote sensing could greatly help in this arena, but we have lacked a clear pathway for interpreting remote sensing signatures in the context of invasive species and biodiversity. The spectra express the biochemical and structural properties of the vegetation, but translating that to species composition requires an increased understanding of the spectral separability of species at different levels of ecological and taxonomic aggregation.

We presented a study of the spectral separability of the most common tree species found in tropical and subtropical forests of Hawai'i. Our goal was to assess if and how mature tree canopies are statistically unique in their spectral signatures. We then made a first attempt to associate the observed differences in spectral signatures with their leaf biochemical and canopy structural properties. Our work provides the following conclusions and considerations:

- Hawaiian native trees are generally unique from those of introduced trees by way of their reflectance, first-derivative, and second-derivative spectral properties. N-fixing trees, be they native or introduced, are spectrally unique from other groups of non-fixing trees.
- Species deemed to be highly invasive are spectrally separable from the introduced species that do not proliferate across Hawaiian ecosystems. These differences are expressed in the shortwave-IR spectrum associated with upper-canopy water content and architecture.
- The observed differences in canopy spectral signatures are linked to relative differences in leaf pigment (chlorophyll, carotenoids), nutrient (N, P), and structural (SLA) properties, as well as to canopy LAI. These leaf and canopy properties contribute in different ways to the spectral properties of the trees, with wavelength-specific reflectance and absorption features that overlap but which are spectrally unique from one another.
- SLA contributes uniquely to the shortwave-IR (1500–2500 nm) reflectance properties of densely foliated canopies. This may allow for detection of SLA variations across rainforest canopies, thereby allowing for spatially-explicit analyses of canopy function and ecosystem processes.
- Critically, the spectral separability of Hawaiian native and introduced tree species varies by measurement type (reflectance, 1st-deriv, 2nd-deriv) and with the composition of the groups being compared. There is no single spectral region that always defines the separability of the species groups, and thus the full-range (400–2500 nm) spectrum is required to accommodate the differing spectral relationships between species.

This study sets the basis for a new invasive species monitoring program in Hawai'i using imaging spectroscopy as a key technology. It also provides direction for future studies of species composition and biodiversity. Algorithms developed for invasive species monitoring should focus on the spatial scale of analysis, combined with the biochemical and structural properties of the targeted species. Although this initial study does not address issues of tree size or canopy development stage, and does not attempt to map native and invasive species in Hawai'i, the basic spectral separability of the major groups of species appears tractable and ready for further investigation. Our forthcoming efforts will focus on these issues.

Acknowledgements

We thank C. Perry, K. Carlson, R. Ostertag, H. Farrington, and G. Sanchez for field assistance. We thank D. Turner and P. Vitousek for assistance with leaf nutrient analysis. We thank M. Eastwood, R. Green, and the AVIRIS team for airborne data acquisition. We thank D. Muchoney and two anonymous reviewers for helpful comments on the manuscript. Access to field sites was provided by Hawaii Division of Forestry and Wildlife, Hawaii Army National Guard, and Kamehameha Schools. This work was supported by NASA Terrestrial Ecology and Biodiversity Program grant NNG-06-GI-87G, The Carnegie Institution, and the U.S. Forest Service.

Appendix A. Mean leaf biochemical, SLA and canopy LAI properties of all species

Location	Species	Chl-a ($\mu g/cm^2$)	Chl-b ($\mu g/cm^2$)	Carotenoids ($\mu g/cm^2$)	N (%)	P (%)	N (g/m^2)	P (g/m^2)	SLA (cm^2/g)	H_2O (%)	EWT (mm)	LAI (m^2/m^2)
HAVO and volcano	*Acacia koa*	50.46	17.21	15.79	2.680	0.113	6.21	0.26	43.19	54.93	0.28	2.51
	Cryptomeria japonica	29.13	9.95	9.10	1.015	0.276	2.20	0.60	46.06	63.30	0.37	3.57
	Eucalyptus globulus	41.07	14.73	12.75	1.46	0.12	2.81	0.23	51.93	55.76	0.243	3.41
	Fraxinus uhdei	22.86	7.64	10.54	1.256	0.148	1.76	0.21	71.48	55.07	0.172	4.92
	Juniperus bermudiana	28.40	11.69	8.54	0.820	0.105	1.13	0.14	72.58	61.25	0.22	3.23
	Magnolia grandiflora	36.28	13.03	13.20	1.115	0.121	2.19	0.24	50.87	53.57	0.227	3.78
	Metrosideros polymorpha	40.44	15.34	12.37	0.69	0.06	1.79	0.15	38.85	50.57	0.26	3.13
	Morella faya	53.39	20.29	18.24	1.71	0.05	3.00	0.09	57.22	51.67	0.19	7.13
	Myrsine lessertiana	43.05	15.66	13.54	1.340	0.119	1.71	0.15	78.44	66.96	0.258	2.48
	Nestegis sandwicensis	33.79	13.42	11.86	1.081	0.084	1.68	0.13	64.24	51.40	0.165	3.72
	Pisonia brunoniana	31.40	12.72	11.61	0.936	0.080	1.32	0.11	70.90	56.11	0.180	3.45
	Podocarpus neriifolius	18.17	6.69	7.31	1.187	0.266	1.55	0.35	76.70	64.33	0.235	4.46
	Sapindus saponaria	50.82	18.95	16.75	3.343	0.202	2.62	0.16	127.69	63.29	0.135	3.96
	Tibouchina granulosa	22.79	7.51	8.87	1.204	0.140	1.47	0.17	81.68	68.33	0.264	3.28
Puna, lava tree and KMR	*Casuarina equisetifolia*	27.33	9.70	9.30	1.368	0.074	1.85	0.10	73.79	66.38	0.27	2.84
	Cecropia obtusifolia	27.43	9.16	8.08	2.35	0.14	1.99	0.12	118.19	70.45	0.20	3.45
	Diospyros sandwicensis	34.44	13.08	11.33	1.09	0.08	1.87	0.13	60.37	52.64	0.19	2.48
	Eucalyptus deglupta	14.41	3.80	6.07	0.962	0.087	1.46	0.13	65.83	51.96	0.164	3.29
	Falcataria moluccana	37.70	10.35	9.47	2.94	0.09	2.75	0.08	108.60	56.60	0.12	3.43
	Ficus benjamina	17.02	5.05	7.61	1.103	0.089	1.61	0.13	68.37	57.91	0.201	5.49
	Ficus elastica	38.51	14.07	12.52	1.304	0.147	2.55	0.29	51.23	71.97	0.501	3.79
	Ficus microcarpa	41.47	14.80	14.70	1.354	0.096	2.06	0.15	65.59	50.41	0.155	5.84
	Ficus microcarpa	43.88	17.10	14.02	1.398	0.103	2.03	0.15	69.01	53.84	0.169	7.27
	Macaranga mappa	33.56	13.22	10.05	1.39	0.08	1.41	0.08	110.29	64.27	0.18	3.03
	Mangifera indica	18.77	5.83	6.66	0.829	0.107	1.21	0.16	68.59	56.44	0.19	5.29
	Melastoma candidum	29.80	12.23	7.69	1.55	0.08	0.99	0.05	159.65	68.50	0.14	5.10
	Metrosideros polymorpha	29.77	10.88	9.41	0.86	0.05	1.71	0.10	51.25	52.99	0.22	2.14
	Metrosideros polymorpha	38.84	14.35	11.83	0.95	0.06	1.86	0.12	50.88	53.12	0.22	2.89
	Psidium cattleianum	43.64	18.67	12.92	1.02	0.05	1.59	0.08	64.30	59.00	0.22	3.72
	Schefflera actinophylla	37.48	15.57	11.95	0.939	0.103	1.93	0.21	48.72	60.26	0.311	3.78
	Trema orientalis	29.92	10.47	9.47	3.105	0.233	2.10	0.16	147.53	69.77	0.156	5.44
	Trema orientalis	39.37	12.26	12.28	2.658	0.163	2.46	0.15	108.16	66.74	0.186	3.50
Pu‘u Wa‘awa‘a	*Grevillea robusta*	30.72	11.54	12.48	1.103	0.062	1.87	0.10	59.13	47.44	0.153	3.44
	Metrosideros polymorpha	43.09	16.98	13.22	0.846	0.067	1.96	0.16	43.08	52.21	0.254	2.30
	Schinus molle	44.02	14.84	14.90	1.854	0.198	2.43	0.26	76.30	61.76	0.212	2.85
Kohala	*Cryptomeria japonica*	29.13	9.95	9.10	1.015	0.276	2.20	0.60	46.06	63.30	0.37	3.58
	Metrosideros polymorpha	36.27	13.39	11.39	1.04	0.09	1.80	0.16	57.76	60.53	0.27	3.10
Laupahoehoe	*Fraxinus uhdei*	38.10	13.35	13.51	1.763	0.135	2.88	0.22	61.28	51.27	0.172	5.58
	Metrosideros polymorpha	56.12	23.18	16.53	1.26	0.08	2.10	0.14	59.94	58.08	0.23	3.48

References

Asner, G. P. (1998). Biophysical and biochemical sources of variability in canopy reflectance. *Remote Sensing of Environment*, *64*, 134−153.

Asner, G. P., Elmore, A. J., Hughes, F. R., & Vitousek, P. M. (2005). Ecosystem structure along bioclimatic gradients in Hawai'i from imaging spectroscopy. *Remote Sensing of Environment*, *96*, 497−508.

Asner, G. P., Martin, R. E., Carlson, K. M., Rascher, U., & Vitousek, P. M. (2006). Vegetation–climate interactions among native and invasive species in Hawaiian rainforest. *Ecosystems*, *9*, 1106−1117.

Asner, G. P., & Vitousek, P. M. (2005). Remote analysis of biological invasion and biogeochemical change. *Proceedings of the National Academy of Sciences*, *102*, 4383−4386.

Asner, G. P., & Warner, A. S. (2003). Canopy shadow in IKONOS satellite observations of tropical forests and savannas. *Remote Sensing of Environment*, *87*, 521−533.

Baruch, Z., & Goldstein, G. (1999). Leaf construction cost, nutrient concentration, and net CO2 assimilation of native and invasive species in Hawaii. *Oecologia*, *121*, 183−192.

Blackburn, G. A., & Steele, C. M. (1999). Towards the remote sensing of matorral vegetation physiology: Relationships between spectral reflectance, pigment, and biophysical characteristics of semiarid bushland canopies. *Remote Sensing of Environment*, *70*, 278−292.

Ceccato, P., Flasse, S., Tarantola, S., Jacquemoud, S., & Gregoire, J. M. (2001). Detecting vegetation leaf water content using reflectance in the optical domain. *Remote Sensing of Environment*, *77*, 22−33.

Chen, S., Hong, X., Harris, C. J., & Sharkey, P. M. (2004). Sparse modeling using orthogonal forest regression with PRESS statistic and regularization. *IEEE Transactions on Systems, Man and Cybernetics*, *34*, 898−911.

Clark, R. N., Swayze, G. A., Livo, K. E., Kokaly, R. F., Sutley, S. J., Dalton, J. B., McDougal, R. R., & Gent, C. A. (2003). Imaging spectroscopy: Earth and planetary remote sensing with the USGS Tetracorder and expert systems. *Journal of Geophysical Research-Planets*, *108*, ISI:000187484400001.

Coops, N. C., Smith, M. -L., Martin, M. E., & Ollinger, S. V. (2003). Prediction of Eucalypt foliage nitrogen content from satellite-derived hyperspectral data. *IEEE Transactions on Geoscience and Remote Sensing*, *41*, 1338−1346.

Crews, T. E., Kitayama, K., Fownes, J. H., Riley, R. H., Herbert, D. A., Mueller-Dombois, D., & Vitousek, P. M. (1995). Changes in soil phosphorus fractions and ecosystem dynamics across a long chronosequence in Hawaii. *Ecology*, *76*, 1407−1424.

Curran, P. J. (1989). Remote sensing of foliar chemistry. *Remote Sensing of Environment*, *30*, 271−278.

D'Antonio, C. M., & Vitousek, P. M. (1992). Biological invasions by exotic grasses, the grass/fire cycle, and global change. *Annual Review of Ecology and Systematics*, *23*, 63−87.

Datt, B. (1998). Remote sensing of chlorophyll a, chlorophyll b, chlorophyll a+b, and total carotenoid content in Eucalyptus leaves. *Remote Sensing of Environment*, *66*, 111−121.

Dawson, J. W., & Stemmermann, L. (1990). *Metrosideros* (Myrtaceae). In W. L. Wagner, D. R. Herbst, & S. H. Sohmer (Eds.), *Manual of the flowering plants of Hawaii*. Honolulu, Hawaii: Bernice P. Bishop Museum.

Durand, L. Z., & Goldstein, G. (2001). Photosynthesis, photoinhibition, and nitrogen use efficiency in native and invasive tree ferns in Hawaii. *Oecologia*, *126*, 345−354.

Ehrenfeld, J. G. (2003). Effects of exotic plant invasions on soil nutrient cycling processes. *Ecosystems*, *6*, 503−523.

Evans, J. R., Vogelmann, T. C., Williams, W. E., & Gorton, H. L. (2004). Chloroplast to leaf. In W. Smith, T. C. Vogelmann, & C. Critchley (Eds.), *Photosynthetic adaptation: Chloroplast to landscape* (pp. 15−41). New York: Springer.

Gitelson, A. A., Zur, Y., Chivkunova, O. B., & Merzlyak, M. N. (2002). Assessing carotenoid content in plant leaves with reflectance spectroscopy. *Photochemistry and Photobiology*, *75*, 272−281.

Grossman, Y. L., Ustin, S. L., Jacquemoud, S., Sanderson, E. W., Schmuck, G., & Verdebout, J. (1996). Critique of stepwise multiple linear regression for the extraction of leaf biochemistry information from leaf reflectance data. *Remote Sensing of Environment*, *56*, 182−193.

Grotkopp, E., Rejmanek, M., & Rost, T. I. (2001). Toward a causal explanation of plant invasiveness: seedling growth and like-history strategies of 29 pine (*Pinus*) species. *The American Naturalist*, *159*, 369−419.

Gulias, J., Flexas, J., Mus, M., Cifre, J., Lefi, E., & Medrano, H. (2003). Relationship between maximum leaf photosynthesis, nitrogen content and specific leaf area in Balearic endemic and non-endemic Mediterranean species. *Annals of Botany*, *92*, 215−222.

Herbert, D. A., & Fownes, J. H. (1999). Forest productivity and efficiency of resource use across a chronosequence of tropical montane soils. *Ecosystems*, *2*, 242−254.

Hughes, F. R., & Denslow, J. S. (2005). Invasion by a N_2-fixing tree alters function and structure in wet lowland forests of Hawaii. *Ecological Applications*, *15*, 1615−1628.

Hughes, R. F., Vitousek, P. M., & Tunison, T. (1991). Alien grass invasion and fire in the seasonal submontane zone of Hawai'i. *Ecology*, *72*, 743−746.

Jacquemoud, S., Verdebout, J., Schmuck, G., Andreoli, G., & Hosgood, B. (1995). Investigation of leaf biochemistry by statistics. *Remote Sensing of Environment*, *54*, 180−188.

Li, Y., Demetriades-Shah, T. H., Kanemasu, E. T., Shultis, J. K., & Kirkham, M. B. (1993). Use of second derivatives of canopy reflectance for monitoring prairie vegetation over different soil backgrounds. *Remote Sensing of Environment*, *44*, 81−154.

Lichtenthaler, H. K. (1987). Chlorophyll and carotenoids: Pigments of photosynthetic membranes. *Methods in Enzymology*, *148*, 350−387.

Lichtenthaler, H. K., & Buschmann, C. (2001). Chlorophylls and carotenoids: Measurement and characterization by UV–VIS spectroscopy. *Current protocols in food analytical chemistry* (pp. F4.3.1−F4.3.8). New York: John Wiley and Sons.

Loope, L. L., & Mueller-Dombois, D. (1989). Characteristics of invaded islands, with special reference to Hawaii. In J. Drake, F. DiCastri, R. Groves, F. Kruger, H. A. Mooney, M. Rejmanek, & M. Williamson (Eds.), *Biological invasions: A global perspective* (pp. 257−280). Chichester: Wiley and Sons.

Martin, M. E., & Aber, J. D. (1997). High spectral resolution remote sensing of forest canopy lignin, nitrogen, and ecosystem processes. *Ecological Applications*, *7*, 431−444.

Myneni, R. B., Ross, J., & Asrar, G. (1989). A review on the theory of photon transport in leaf canopies. *Agricultural and Forest Meteorology*, *45*, 1−153.

Niinemets, U., Portsmuth, A., & Truus, L. (2002). Leaf structural and photosynthetic characteristics, and biomass allocation to foliage in relation to foliar nitrogen content and tree size in three Betula species. *Annals of Botany (London)*, *89*, 191−204.

Reich, P. B., Walters, M. B., & Ellsworth, D. S. (1997). From tropics to tundra: Global convergence in plant functioning. *Proceedings of the National Academy of Sciences*, *94*, 13730−13734.

Rejmánek, M., Richardson, D. M., Higgins, S. I., Pitcairn, M. J., & Grotkopp, E. (2005). Ecology of invasive plants: State of the art. In H. A. Mooney, R. N. Mack, J. A. McNeely, L. E. Neville, P. J. Schei, & J. K. Waage (Eds.), *Invasive alien species: A new synthesis* (pp. 104−161). Washington, DC: Island Press.

Sax, D. F., Gaines, S. D., & Brown, J. H. (2002). Species invasions exceed extinctions on islands worldwide: A comparative study of plants and birds. *The American Naturalist*, *160*, 766−783.

Sims, D. A., & Gamon, J. A. (2002). Relationships between leaf pigment content and spectral reflectance across a wide range of species, leaf structures and developmental stages. *Remote Sensing of Environment*, *81*, 337−354.

Smith, M. L., Martin, M. E., Plourde, L., & Ollinger, S. V. (2003). Analysis of hyperspectral data for estimation of temperate forest canopy nitrogen concentration: Comparison between an airborne (AVIRIS) and spaceborne (Hyperion) sensor. *IEEE Transactions on Geoscience and Remote Sensing*, *41*, 1332−1337.

Stemmermann, L. (1983). Ecological studies of Hawaiian Metrosideros in a successional context. *Pacific Science*, *37*, 361−373.

Ustin, S. L., Roberts, D. A., Gamon, J. A., Asner, G. P., & Green, R. O. (2004). Using imaging spectroscopy to study ecosystem processes and properties. *Bioscience*, *54*, 523−534.

Vitousek, P. M. (2004). *Nutrient cycling and limitation: Hawai'i as a model system.* Princeton, NJ: Princeton University Press.

Vitousek, P. M., D'Antonio, C. M., Loope, L. L., Rejmanek, M., & Westbrooks, R. (1997). Introduced species: A significant component of human-caused global change. *New Zealand Journal of Ecology*, *21*, 1−16.

Vitousek, P. M., & Walker, L. R. (1989). Biological invasion by Myrica faya in Hawai'i: Plant demography, nitrogen fixation, ecosystem effects. *Ecological Monographs*, *59*, 247−265.

Vitousek, P. M., Walker, L. R., Whiteacre, L. D., Mueller-Dombois, D., & Matson, P. A. (1987). Biological invasion by *Myrica faya* alters ecosystem development in Hawaii. *Science*, *238*, 802−804.

Wagner, W.L., Herbst, D.R., & Sohmer, S.H. (1999). *Manual of the flowering plants of Hawai'i*. Honolulu: University of Hawaii Press and Bishop Museum Press.

Welles, J. M., & Norman, J. M. (1991). Instrument for indirect measurement of canopy architecture. *Agronomy Journal*, *83*, 818−825.

Wessman, C. A., Aber, J. D., Peterson, D. L., & Melillo, J. M. (1988). Remote sensing of canopy chemistry and nitrogen cycling in temperate forest ecosystems. *Nature*, *335*, 154−156.

Wright, I. J., Reich, P. B., Cornelissen, J. H. C., Falster, D. S., Garnier, E., Hikosaka, K., Lamont, B. B., Lee, W., Oleksyn, J., Osada, N., Poorter, H., Villar, R., Warton, D. I., & Westoby, M. (2005). Assessing the generality of global leaf trait relationships. *New Phytologist*, *166*, 485−496.

Yamashita, N., Ishida, A., Kushima, H., & Tanaka, N. (2000). Acclimation to sudden increase in light favoring an invasive over native trees in subtropical islands, Japan. *Oecologia*, *125*, 412−419.

Yoder, B. J., & Pettigrew-Crosby, R. E. (1995). Predicting nitrogen and chlorophyll content and concentrations from reflectance spectra (400–2500 nm) at leaf and canopy scales. *Remote Sensing of Environment*, *53*, 199−211.

Zar, J. H. (1999). *Biostatistical analysis.* New Jersey: Prentice Hall.

Zarco-Tejada, P. J., Miller, J. R., Noland, T. L., Mohammed, G. H., & Sampson, P. H. (2001). Scaling-up and model inversion methods with narrowband optical indices for chlorophyll content estimation in closed forest canopies with hyperspectral data. *IEEE Transactions on Geoscience and Remote Sensing*, *39*, 1491−1507.